ELSEVIER

1 October 1996

Optics Communications 130 (1996) 385–392

OPTICS COMMUNICATIONS

Full length article

Interactions of optical vortex solitons superimposed on different background beams

I. Velchev, A. Dreischuh *, D. Neshev, S. Dinev

Department of Quantum Electronics, Sofia University, 5, J. Bourchier Blvd., BG-1126 Sofia, Bulgaria

Received 6 March 1995; revised version received 11 December 1995; accepted 18 January 1996

Abstract

The interaction between two optical vortex solitons (OVS), formed on different background beams is analyzed numerically. Analogous to the one-dimensional case, vector OVS seem obtainable [12]. The relative topological charges of the interacting (off-axis) vortices are found to rule their propagation characteristics. Attraction is found in the case of equal charges, in contrast to the opposite case, where repulsion is present.

1. Introduction

Optical vortices are characterized as two-dimensional screw dislocations on a plane wavefront. They can be nested in the output beams of slightly detuned laser cavities with large Fresnel numbers [1]. The unusual angular optical phase ramp could be produced experimentally by illuminating a proper spiral-phase delay-plate [2] or by diffraction on computer-synthesized gratings [3,4]. The existence of such a dislocation requires that the amplitude of the electric field becomes zero at the dislocation center. From the mathematical point of view, the screw phase dislocation is described by the multiplier $\exp(\mathrm{i}m\varphi)$, where φ is the azimuthal coordinate and m is an odd number ensuring a $(m\pi)$ diametrical phase jump, which sign determines the direction of the dislocation. The counterclockwise direction ($m > 0$) is known to be a positive "topological charge" $(+m)$ [5]. In this paper we investigate formations with topological charges of ± 1, which determine the $\pm 2\pi$ phase variance in the azimuthal direction.

The free-space propagation of a TEM_{00} laser beam passed through a spiral phase-plate with a 2π phase ramp leads to a beam-reshaping into a helix [6]. Multiple vortices of the same topological charge are known to propagate linearly retaining their relative positions and their positions within the host beam [4,7]. In contrast, vortices of opposite charges attract each other [4,7], which could lead to their annihilation.

The first observations of optical vortices in a self-defocusing medium, where the field propagates as a soliton, as a consequence of the balance between the diffraction and the nonlinearity, are reported in Ref. [8]. Optical vortex solitons (OVS) are generated presently by a phase mask of regions of uniform phase retardation [8], by initiating an instability of one-dimensional dark soliton stripes with respect to long-period perturbations [9]. The spatial guiding of

* Corresponding author. Fax: +35 92 463589; E-mail: aldrei@phys.uni-sofia.bg.

PII S0030-4018(96)00085-5

a probe beam by an OVS is observed [8] and makes reasonable novel all-optical guiding and switching schemes to be analyzed.

Analyses on interactions of OVSs in two transverse dimensions along the nonlinear medium ((2 + 1)D interactions) are already in progress. It was shown numerically [5], that points and lines of phase discontinuity can evolve in regular crystals of nonlinear vortices. Rotation of an off-axis vortex around the beam axis should be expected too [5]. In a recent experiment [10], rotation of a pair of off-axis OVS with unit topological charge along a nonlinear medium is observed. The sensitivity of the rotation angle with respect to the background intensity could allow a rotary all-optical switch to be constructed.

In this work we analyzed numerically different interaction configurations involving OVSs, formed on different backgrounds. In some cases (vector OVS, composed of a pair of partial OVSs; radiation, caused by on-axially interacting fundamental OVSs) a complete qualitative analogy to the 1D case is found [11,12]. Both attraction and repulsion between axially offset OVSs are observed during the calculations. It is found, that the regime of interaction depends crucially on the OVSs' topological charges, whereas the interaction strength is sensitive to the cross-phase modulational (XPM) coupling between the two beams.

2. Numerical model

The spatial self-action and the XPM coupling of 2D optical beams along the nonlinear medium are described by the incoherently coupled Schrödinger equations

$$i\frac{\partial U}{\partial \xi} + \tfrac{1}{2}\nabla^2 U + R_U\left[|U|^2 + \sigma |V|^2\right] = 0, \qquad (1a)$$

$$i\frac{\partial V}{\partial \xi} + \tfrac{1}{2}\nabla^2 V + R_V\left[|V|^2 + \sigma |U|^2\right] = 0, \qquad (1b)$$

where $U(x, y, \xi)$ and $V(x, y, \xi)$ are the slowly varying beam envelopes, $\nabla^2 = \partial^2/\partial x^2 + \partial^2/\partial y^2$, $R_{U,V}$ denotes the ratio between the nonlinear and the diffraction lengths for each beam. The XPM coefficient σ depends on the ellipticities of the beam polarizations. Self-defocusing nonlinear media are required for the formation of dark spatial solitons. Therefore, $R_{U,V}$ should be negative. For simplicity, we assumed $R_{U,V} = -1$, i.e. equal diffraction and nonlinear lengths for each beam. The nonlinear length for the ith beam is inversely proportional to its background intensity. Assuming equal initial HW1e for each dark beam we can scale the longitudinal coordinate in units of diffraction length. All our computer simulations are based on 2D generalization of the split-step Fourier method expanded over 256 $\times$ 256 grid points. Under these conditions an axial offset of $\Delta = 0.5$ between the interacting OVSs (Section 3.3) corresponds to the separation between the nth and $(n + 2)$th point of the grid.

3. Results and discussion

3.1. Vector optical vortex solitons

Its is shown in Ref. [12], that 1D optical vector dark solitons should exist as bond states of pairs of gray solitons coupled by XPM. Exact solutions of Eq. (1) in 1D are found for $\sigma = 1$. In order to check the accuracy of our numerical routine, we modeled this 1D interaction [12], choosing the background intensities 2 times lower than the required (due to the existence of soliton constant [11,13]) for a fundamental 1D odd dark spatial soliton. In the absence of XPM, each of these 1D dark beams was found to evolve in an 1D odd dark spatial soliton (ODSS) with a $\sqrt{2}$ times larger width. At $\sigma = 1$ we observed the proposed bond-state formation of two partial 1D ODSS, called 1D vector soliton.

We modeled this situation in 2D with an initial condition

$$U(\xi = 0, r, \varphi) = V(\xi = 0, r, \varphi) = B(r)\tanh(\sqrt{2}\, r)\exp(i\varphi), \qquad (2a)$$

where the background $B(r)$ has a super-Gaussian profile:

$$B(r) = A_0 \exp\left[-\tfrac{1}{2}(r/18)^{10}\right]. \qquad (2b)$$

These assumptions follow the single optical vortex approximation from Ref. [8]. The background intensity for generation of OVS is $\sqrt{2}$ times higher than

the required for achieving a 1D odd dark spatial soliton (see the text after Eq. (2) in Ref. [8]). Physically, this result could be attributed to the higher diffraction in two spatial dimensions as compared to that in the 1D case. The multiplier $\sqrt{2}$ in the argument of hyperbolic tangent (Eq. (2a)) describes odd dark beams with radii $\sqrt{2}$ times shorter than those, required to form fundamental OVSs in the absence of XPM. This is a strict 2D generalization of the interaction configuration from Ref. [12].

At $\sigma = 1$ we observed the formation of a vector 2D OVS composed of two partial OVSs of equal topological charges. Fig. 1 shows two gray-scale images of one of the two identical odd dark beams at $\xi = 0$ (Fig. 1a) and $\xi = 3$ (Fig. 1b). Despite strong background spreading both the intensity and phase distribution remain unchanged in the dark beam area. Because of the increasing computational inaccuracy, as a consequence of background spreading, we have restricted our simulations to $\xi = 5.5$. Such a distance of propagation seems satisfactory to conclude that a vector OVS does exist. At this point the analysis of Law and Swartzlander [14] should be referred. In particular, the authors have found that the XPM may destabilize all other modes except those with a circular polarization. Special attention to this problem will be paid in Section 3.3.

3.2. Secondary dark ring solitons

If the background amplitude is not high enough, the input 1D odd dark formation evolves into an 1D odd dark soliton of increased width, corresponding to the soliton constant. If the amplitude is higher, the input 1D odd dark beam evolves into a fundamental 1D ODSS, generating a diverging pair of secondary gray solitons [11,15].

In our numerical simulations we considered two fundamental OVSs

$$U(\xi = 0,\ r,\ \varphi) = V(\xi = 0,\ r,\ \varphi) = B(r)\ \tanh(r)\ \exp(i\varphi), \qquad (3a)$$

formed onto different background beams with super-Gaussian profiles

$$B(r) = A_0 \exp\left[-\tfrac{1}{2}[r/18]^{10}\right]. \qquad (3b)$$

In the presence of XPM the evolution of each beam is influenced by the second one. In a certain sense, this coupling is equivalent to background intensity enhancement of a single beam. Fig. 2 demonstrates the numerical results obtained by solving Eq. (1) with initial conditions, given by Eqs. (3) at $\sigma = 2$. Because of their symmetry, the evolution of both beams is complete identical. The input 2D optical vortex (Fig. 2a) evolves in a 2D OVS coupled to a second one on its own background. The

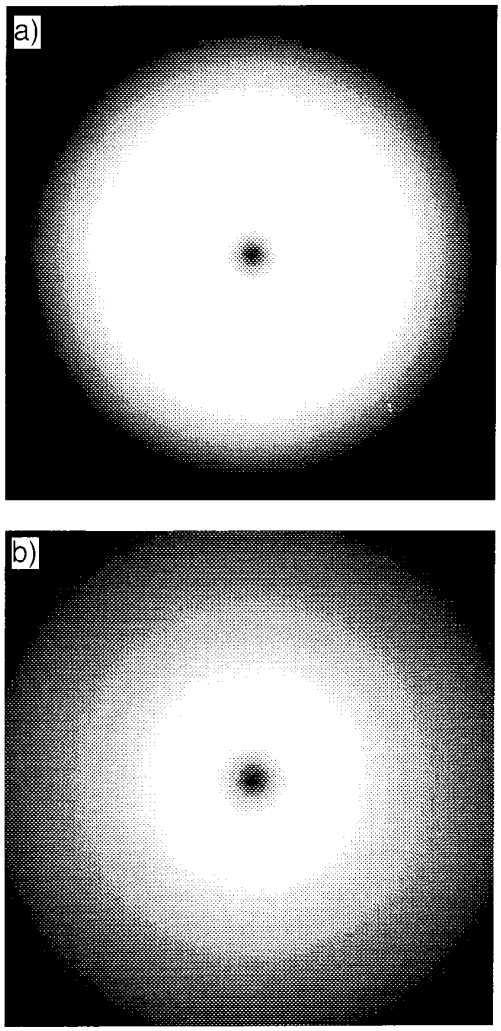

Fig. 1. Gray-scale image of one of the partial OVSs from the vector OVS ($\sigma = 1$) at the entrance $\xi = 0$ of the nonlinear medium (a) and at $\xi = 3$ (b).

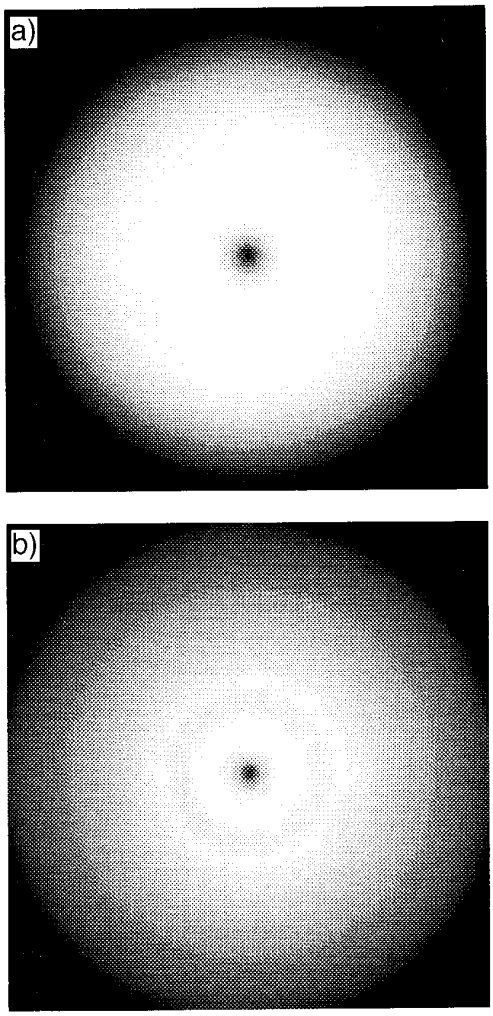

Fig. 2. Splitting of a fundamental OVS, coupled to a second OVS on a different background ($\sigma = 2$): (a) $\xi = 0$, (b) $\xi = 4$. The evolution of the second beam is identical to that of the first one.

excessive "lack of energy" (in view of the XPM coupling and the dark beam radii) leads to the formation of a diverging (along the nonlinear medium) gray ring. As the dark-ring diameter increases (Fig. 2b – $\xi = 4$), the contrast reduces, due to the conservation of the "lack of energy". In the phase domain, the π jump at the center of each dark beam remains undistorted by the XPM. Small ($\sim \pi/5$) phase jumps in each diametrical slice of the dark ring were observed. Therefore, this ring formation could be classified as an optical ring dark soliton [16] generated from odd initial conditions (Eq. (3)).

3.3. Interaction between offset OVSs

It is shown, that in one transverse dimension, the odd dark solitons, composing the vector dark soliton, are strongly coupled due to their mutual trapping [12]. In two transverse dimensions this type of interaction was modeled by solving Eq. (1) for the initial field distribution as presented in Eq. (3), the center of the second OVS being offset from the first one by Δ along the x-axis,

$$U(x, y, \xi = 0) = V(x + \Delta, y, \xi = 0). \qquad (4)$$

At $\Delta \approx 1.5$ we observed reshaping and guiding of a part of each background by the OVS superimposed onto the other one. Due to the decreased dark beam overlapping, an interaction between OVSs was not clearly expressed. A part of the subsequent analyses refets to the value $\Delta = 0.5$. Special attention should be paid to the topological charges of the interacting vortices.

Let us assume that $\sigma = 1$. An interaction can involve two offset OVSs (Fig. 3a upper row) of equal topological charges (Fig. 3a lower row). The transverse phase distribution is presented as gray-scale image, where white denotes $\varphi = 2\pi$, while black indicates $\varphi = 0$. In Fig. 3b the corresponding transverse intensity (upper row) and phase (lower row) distributions after propagation up to a distance $\xi = 3$ are shown. The background self-action influences the phase distribution at larger r. The radial asymmetry in the interaction of 2 OVSs at $\Delta \neq 0$ leads to the formation of spiral structures on the backgrounds around each of the dark beams. The important effect, namely the change of Δ along the longitudinal coordinate ξ, is much better expressed in Fig. 4. Diametrical slices of the OVSs along the x-axis (see Eq. (4)) are presented for $\xi = 0$, up to $\xi = 9$. Because of their different backgrounds, the question, do they pass through each other, or are they reflected off each other is reasonable [17]. In order to answer this question we plotted the intensity slice of the initially "left" vortex with a dashed line. It is seen that both dark beams are overlapped at $\xi = 3$ and, thereafter, they reach maximum separa-

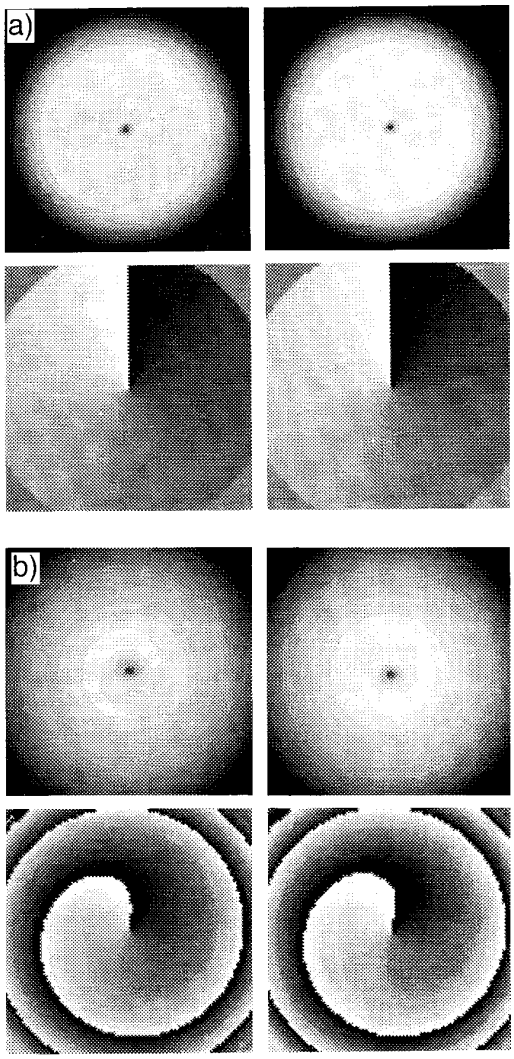

Fig. 3. (a) Gray-scale images of the intensity (upper row) and phase (lower row) distributions of off-axially interacting 2D partial OVSs with equal topological charges at $\xi = 0$ ($\Delta = 0.5$, $\sigma = 1$). (b) The same as (a) at $\xi = 3$.

tion at $\xi = 6.5$. Then, due to mutual attraction, they overlap themselves at $\xi = 9$. This oscillatory behavior repeats along the propagation. At this point one should note, that in the linear regime of propagation, optical vortices of equal topological charges, formed upon a common background do not change their relative positions, as well as their positions with respect to the background [4,7].

Consequently, in contrast to the linear regime, an attractive force between two OVSs with equal topological charges is present.

Let us consider the interaction between two OVSs having initial offset $\Delta = 0.5$ (see Eq. (4)) and $\sigma = 1$ (Fig. 3a upper row). The assumption of opposite topological charges (Fig. 5a) was proven to change generally the interaction. We investigate the nonlinear evolution of both beams (coupled by XPM) up to distance $\xi = 3$, at which they do overlap in the case of equal topological charges (see Fig. 4). The intensity distributions at $\xi = 3$ are presented in Fig. 5b for both beams. The intensity profiles exhibit again spiral structure on the background, but the most important result, is that attraction between the OVSs with opposite charges is absent (Fig. 6). It should be noticed, however, that the linear propagation of optical vortices of opposite charges, localized on a common background, is known to lead to mutual attraction and, eventually, to collision and annihilation [7].

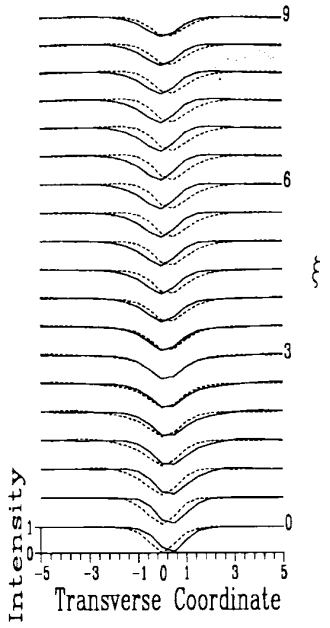

Fig. 4. Evolution of the transverse x-slices of the interacting ($\sigma = 1$) offset OVSs with equal topological charges. An attraction is clearly expressed.

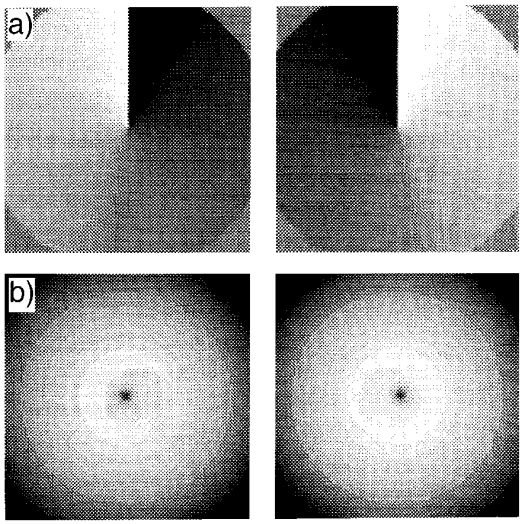

Fig. 5. (a) Gray-scale images of the phase distributions of off-axially interacting 2D partial OVSs with opposite topological charges at $\xi = 0$ ($\Delta = 0.5$, $\sigma = 1$). (b) The same as Fig. 3a at opposite topological charges and $\xi = 3.2$.

The assumption $\sigma = 1$ was made to retain the closest possible similarity between the 1D results of other authors [12] and the present ones in 2D. We also have investigated the nonlinear evolution of two OVSs having an initial off-axis separation $\Delta(\xi = 0) = 0.5$ in the case of $\sigma = 2$. The XPM becomes stronger and the backgrounds do spread at shorter distances ($\xi = 5$). In the case of equal topological charges, the OVSs overlap (at $\xi = 2.5$), pass through each other and tend to overlap again at $\xi = 5$, instead of $\xi = 3$ and $\xi = 9$, respectively (Fig. 4). The strong nonlinear modulation forces the vector OVSs to radiate the excessive "lack of energy" in the form of spiral structures on the background similar to those in Fig. 3b (upper row). Nevertheless, phase jumps of a low contrast ($\sim \pi/5$ or less) were observed to be centered with respect to the minimum along each diametrical slice. Again vortices of opposite topological charges demonstrated repulsion.

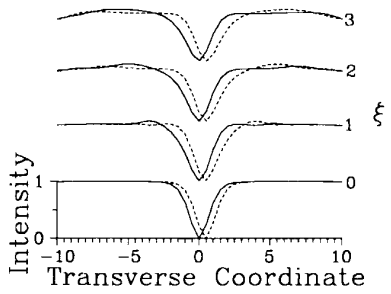

Fig. 6. Evolution of the transverse x-slices of the interacting ($\sigma = 1$) offset ($\Delta = 0.5$) OVSs with opposite topological charges. No attraction is evident.

The nontrivial result on the dependence of the interaction of axially offset OVSs on their relative topological charge was confirmed at various initial offsets $\Delta(\xi = 0)$ ranging from 0.5 to 3.75. The discretization of Δ in units of 0.25 is a result of the computing resources available (see Section 2). In Fig. 7 we plot the dependences of the nonlinear propagation path lengths ξ_1, at which (within the discretization used) attraction or repulsion becomes evident for the first time versus $\Delta(\xi = 0)$. Triangles and dots indicate the numerical data obtained at $\sigma = 2$ and opposite, respectively equal, topological charges. With squares we plot the same dependence for OVSs of equal charges at $\sigma = 1$. Most probably due to the reduced XPM coupling at $\sigma = 1$, OVSs of opposite charges were found not to change their relative positions up to $\xi = 3$ (see Fig. 6). The curves plotted in Fig. 7 represent polynomial fits of the data numerically obtained. The optimal initial OVS offset $\Delta(\xi = 0)$, at which attraction/repulsion becomes evident after the shortest propagation path ξ_1, seems to

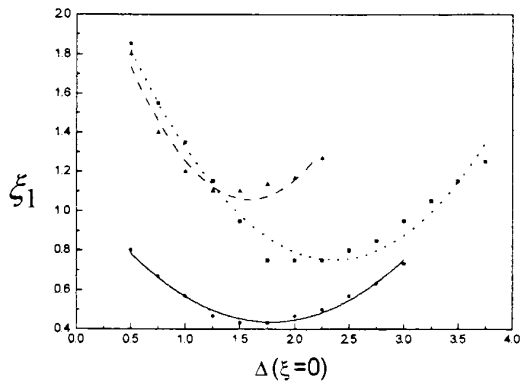

Fig. 7. Nonlinear propagation path length ξ_1, at which OVS attraction/repulsion becomes evident, as a function of the initial off-axial separation Δ (dots and solid line $m = +1$ and $\sigma = 2$; triangles and long-dashed line $m = -1$ and $\sigma = 2$; squares and short-dashed line $m = +1$ and $\sigma = 1$).

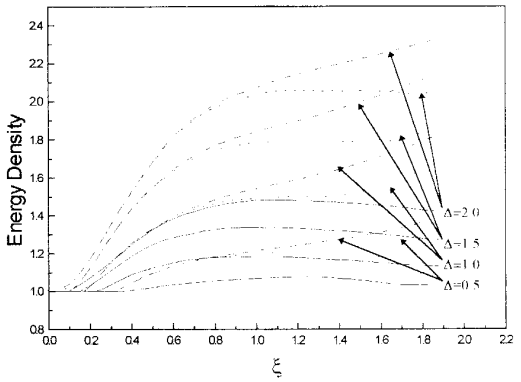

Fig. 8. Energy density of the background peak formed by the OVS through XPM versus nonlinear propagation path length ξ. (Solid curves) $m = +1$, $\sigma = 1$; (short-dashed) $m = +1$, $\sigma = 2$; (long-dashed) $m = -1$, $\sigma = 2$. The values of $\Delta(\xi = 0)$ are given as a parameter.

be within the range 1.5–1.75 at $\sigma = 2$ (see the solid and long-dashed curves in Fig. 7). The corresponding short-dashed curve for OVSs of equal charges propagating with $\sigma = 1$ seems shifted and the optimal OVS-offset seems to be $\Delta(\xi = 0) = 2.0$–2.25. In our opinion this difference could not be attributed to the numerical inaccuracies of the model and should be further analyzed.

As shown in Ref. [8], the OVSs do obey guiding properties. At a nonzero initial offset Δ between the solitons their mutual attraction or repulsion is accompanied with the formation of spiral structures superimposed on the backgrounds (Fig. 3b, upper row, and Fig. 5b). Each one of the OVSs starts to redistribute the energy of the background of the copropagating beam. In Fig. 8 we plot the evolution of the peak energy density of the background beam being guided by the OVS formed onto the other beam versus the nonlinear propagation path length. The solid curves refer to $m = +1$ and $\sigma = 1$, the short-dashed curves to $m = +1$ and $\sigma = 2$, whereas the long-dashed curves demonstrate the results obtained for OVSs of opposite topological charges with $\sigma = 2$. The initial offset $\Delta(\xi = 0)$ is used as a parameter. At a XPM strength $\sigma = 1$ the peaks formed onto the backgrounds tend to grow initially (up to $\xi = 1$ for $\Delta = 2$) and, thereafter, their peak energy density starts decreasing. Practically the same was observed at opposite topological charges $m = -1$ and $\sigma = 1$. As concluded in Ref. [14], the XPM at $\sigma = 2$ destabilizes the off-axial OVS propagation mode for both types of topological charges. At $m = +1$ (i.e. at mutual attraction) the peak guided by the complementary OVS does grow initially saturating approximately in the interval $0.8 < \xi < 1.6$, starting, thereafter, to grow again (Fig. 8, short-dashed curves). The existence of a plateau could be explained by the overlapping (at $\xi = 1.2$) of the beams being mutually attracted and by the small amount of energy to become guided additionally. When the vortices pass through each other the energy density of the peak formed starts to grow faster (Fig. 8, short-dashed curves at $\Delta = 0.5$, 1 and 1.5 at $\xi > 1.6$).

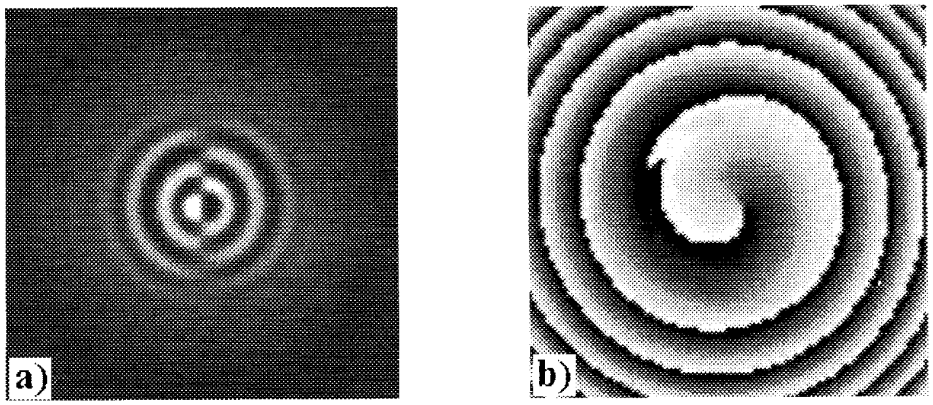

Fig. 9. Intensity (a) and phase (b) portrait of one of the OVSs at a propagation path $\xi = 8$ corresponding to a saturation of the intensity of the bright peak being guided.

It is natural to expect that the peak will saturate at each subsequent overlapping of the OVSs.

The behavior of those pairs of background beams which appear to be guided by the OVS formed onto the complementary beam is more dramatic at $\sigma = 2$ and equal topological charges. This mode of propagation corresponds to a mutual repulsion between the OVSs. Therefore, each OVS will "see" high-intensity parts of the second background and it could be expected to guide even more and more energy. The long-dashed curves on Fig. 8 clearly express this tendency. Saturation of the intensities of the bright peaks could be expected too, since the reduced OVS-overlapping (at an increasing Δ versus ξ) should slow down their repulsion.

In Fig. 9 we plot the intensity (a) and phase (b) portrait of one of the OVSs at $\xi = 8$. Qualitatively, the portrait of the complementary OVS could be obtained by inverting Fig. 9a and by reversing the topological charge shown in Fig. 9b. These two figures correspond to the case described above, i.e. the saturation of the bright peak being guided by the OVS formed on the second background beam. The OVSs seen in the neighborhood of the bright peaks become slightly deformed along the interaction axis. Nevertheless, no reversal of their topological charges is evident. This motivates us to denote the formation of the bright spiral (at moderate propagation distances) and the bright peaks on the backgrounds as parts of the backgrounds being guided by the OVSs. In a certain sense (see Fig. 8) this behavior could be referred to as a saturating modulational instability of the backgrounds at an off-axis propagation of OVSs under a relatively strong XPM.

4. Conclusion

We have shown numerically that in many aspects, the interaction of optical vortex solitons, formed on different background beams, is qualitatively analogous to the interaction between 1D dark odd solitons. The relative topological charge of the off-axially interacting OVSs if found to be a key factor for observing an attraction/repulsion between the dark beams. Further analyses are required to obtain the necessary conditions for generating a spatially stable bundle of OVSs on a common background beam.

Acknowledgements

This work was made possible by financial support from the National Science Found, Bulgaria, under contract #F424/1994.

References

[1] P. Coullet, L. Gil and F. Rocca, Optics Commun. 73 (1989) 403.
[2] S. Tidwell, G. Kim and W. Kimura, Appl. Optics 32 (1993) 5222.
[3] V. Bazhenov, M. Soskin and M. Vasnetsov, J. Mod. Optics 39 (1992) 585.
[4] I. Basistiy, V. Bazhenov, M. Soskin and M. Vasnetsov, Optics Commun. 103 (1993) 422.
[5] G. McDonald, K. Syed and W. Firth, Optics Commun. 94 (1990) 469.
[6] M. Beijersbergen, R Coerwinkel, M. Kirstensen and J. Woerdman, Optics Commun. 112 (1994) 321.
[7] G. Indebetouw, J. Mod. Optics 40 (1993) 73.
[8] G. Swartzlander, Jr. and C. Law, Phys. Rev. Lett. 69 (1992) 2503.
[9] C. Law and G. Swartzlander, Jr., Optics Lett. 18 (1993) 586.
[10] B. Luther-Davies, R. Powles and V. Tikhonenko, Optics Lett. 19 (1994) 1816.
[11] Yu. Kivshar, IEEE J. Quantum Elektron. 29 (1993) 250.
[12] Yu. Kivshar and S. Turitsyn, Optics Lett. 18 (1993) 337.
[13] G. Allan, S. Skinner, D. Andersen and A. Smirl, Optics Lett. 16 (1991) 156.
[14] C. Law and G. Swartzlander, Chaos, Solitons & Fractals 4 (1994) 1759.
[15] W. Zhao and E. Bourkoff, Optics Lett. 14 (1989) 703.
[16] Yu. Kivshar and X. Yang., Phys. Rev. E 50 (1994) R40.
[17] R. Thurston and A. Weiner, J. Opt. Soc. Am. B 8 (1991) 471.